SOVIET PHYSICS JETP VOLUME 22, NUMBER 5 MAY, 1966

HIGH-FREQUENCY STABILIZATION OF THE SCREW INSTABILITY IN AN ELECTRON-HOLE SEMICONDUCTOR PLASMA. I

V. V. VLADIMIROV

Submitted to JETP editor June 5, 1965

J. Exptl. Theoret. Phys. (U.S.S.R.) 49, 1562-1575 (November 1965)

It is shown that the high-frequency stabilization of the screw instability in a semiconductor is due to waves that are reflected from the ends of the sample. These waves give rise to helical modes with different spatial period along the axis of the sample. The time correlation of modes with spatial period comparable with the length of the sample, due to the high-frequency modulation of the current, is responsible for the stabilization. It is shown that high-frequency stabilization can only be achieved in short samples and certain stabilization criteria are given. The results of this theoretical analysis are in good agreement with experiment.[12] The stabilization mechanism considered here should also be operative in the plasma in the positive column.

1. Two effects were reported in 1958 which did not appear to be related to each other, since the exact nature of the phenomena was not clear. These two effects are the anomalous diffusion observed in the plasma in a positive column in a strong magnetic field, which is accompanied by low-frequency noise (approximately 10^5 cps), reported by Lehnert,[1] and the low-frequency current oscillations (approximately 10^4 cps) in a thin long germanium sample in a strong longitudinal magnetic field described by Ivanov and Ryvkin.[2] The phenomenon observed by Lehnert was explained by Kadomtsev and Nedospasov,[3] who developed the theory of the screw (current convective)[1)] instability of the positive column. This theoretical analysis has received extensive verification.[4]

Glicksman[5] modified this theory and applied it to the electron-hole plasma in a semiconductor and also obtained excellent agreement with experiment.[2,6] Subsequently, a number of experimental and theoretical papers appeared[7-11] which discussed various features of the screw instability in semiconductors and shed a great deal of light on the nature of the instability.[9,11]

The work cited above was followed by the publication of experimental results concerning high-frequency stabilization of the screw (current-convective) instability in semiconductors[12] and in the positive column.[13] The application of a high-frequency current of sufficient amplitude stabilizes the instability. This work has aroused great interest since it provides experimental verification of the possibility of preventing plasma instabilities by means of high-frequency fields. However, the mechanism by which the high-frequency field stabilizes the screw instability in the diffusional regime is not yet clear.

Up to the present time the theoretical analysis of high-frequency stabilization of plasma instabilities has been limited to the case of hydrodynamic perturbations;[14] in large part this analysis has been concerned with the treatment of force equations (dynamic stabilization) because the primary factor responsible for the pertinent instabilities is the inertia of the heavy ions. If a parameter (current, magnetic field) is made to be a periodic function of time, these force equations are reduced to a Mathieu equation or a Hill equation, and the stability criteria for these equations then give the required information on dynamic stabilization.[14] As is well known,[3,5] the equations which describe the diffusional screw (current-convective) instability are first-order equations in time since the inertia of the particles is not important (the development of the instability is determined by the balance between the drift and diffusional flows). Hence, these equations do not lead to the usual Mathieu or Hill equations when the ordinary techniques are applied[14] and the nature of the stabilization mechanism remains unclear.[14]

It will be shown below that the primary feature in high-frequency stabilization of the screw in-

[1)]In the present work, by the screw instability in all cases we mean an instability of the diffusional type which Kadomtsev and Nedospasov[3] called the current-convective instability.

stability in semiconductors is due to the presence, in addition to the primary wave, of waves reflected from the ends of the sample; these waves result in formation of helical modes with different spatial periods along the z axis. The time correlation of these modes in the presence of the rf field can result in stabilization. It will be shown below that the kind of high-frequency stabilization mechanism can also operate in the positive column.

2. To analyze the problem we start with the equation of continuity and the equations of motion for the electrons and holes:

$$\frac{\partial n}{\partial t} + \operatorname{div} n\mathbf{v}_e = Zn,$$

$$\frac{\partial p}{\partial t} + \operatorname{div} p\mathbf{v}_h = Zp, \qquad (2)$$

$$\frac{T_e}{m_e^* n}\nabla n = -[\mathbf{v}_e\boldsymbol{\omega}_{eH}] + \frac{e}{m_e^*}\nabla\varphi - \frac{\mathbf{v}_e}{\tau_e}, \qquad (3)^*$$

$$\frac{T_h}{m_h^* p}\nabla p = [\mathbf{v}_h\boldsymbol{\omega}_{hH}] - \frac{e}{m_h^*}\nabla\varphi - \frac{\mathbf{v}_h}{\tau_h}, \qquad (4)$$

where Z is the coefficient of volume generation of non-equilibrium carriers; n and p are the electron and hole densities respectively; m_e^* and m_h^* are the effective masses for the electrons and holes; T_e and T_h are the temperatures for the electrons and holes (we assume hereinafter $T_e = T_h$); τ_e and τ_h are the relaxation times;

$$\boldsymbol{\omega}_{eH} = e\mathbf{H} / m_e^* c,$$
$$\boldsymbol{\omega}_{hH} = e\mathbf{H} / m_h^* c.$$

We consider a thin cylindrical sample, in which case the nonequilibrium carriers recombine only at the surface (the volume recombination time for the carriers is much longer than the diffusion time $\tau_b \gg a^2/D$). A constant magnetic field is applied in the z-direction. For purposes of simplicity we consider the case of a natural semiconductor (n = p); experimental investigations of rf stabilization of the helical instability in semiconductors [12] have also been carried out in the region of natural conductivity of the germanium samples. The carrier diffusion is assumed to be ambipolar so that the equilibrium distributions of potential and density are given by

$$n_0(r) = n_0 J_0(\beta_0 r), \quad \frac{d\varphi_0}{dr} = \frac{D_e - D_h}{b_e + b_h}\frac{1}{n_0(r)}\frac{dn_0}{dr}, \qquad (5)$$

where

$$\beta = \left(\frac{Z}{D_a}\right)^{1/2}, \quad D_a = \frac{D_e + bD_h}{1+b}, \quad D_i = \frac{T_i\tau_i}{m_i^*},$$

$$b = \frac{b_e}{b_h}, \quad b_i = \frac{e\tau_i}{m_i^*};$$

b_i is the mobility of carriers of type i and D_i is the diffusion coefficient for the carriers. The distributions in (5) are obtained under the assumption that $y_i = b_i H/c \ll 1$. This case is the one of most interest in semiconductors.

The boundary conditions at the surface of the sample are

$$\Gamma = -D_a \frac{\nabla n}{n}\Big|_{r=a} = sn|_{r=a}, \qquad (6)$$

where Γ is the flux due to ambipolar diffusion of the carriers to the surface of the sample and s is the rate of surface recombination for the carriers. Hereinafter the zero subscript will be omitted on the equilibrium quantities.

From (6) we find

$$Gx = J_0(x) / J_1(x), \quad x = \beta_0 a, \quad G = D_a / as. \qquad (7)$$

For a given value of G we can find x and the value of the equilibrium density of carriers at the surface of the sample. When $s \to \infty$ ("dirty" surface) $J_0(x) \to 0$ $(x \to 2.41)$ and the equilibrium density vanishes at the surface. Under these conditions, to a high degree of accuracy[3,5] the radial dependence of the drift quantities can be approximated by the Bessel function $J_1(\beta_1 r)$ where $\beta_1 a$ is the first root of the function J_1, thus allowing a considerable simplification of the problem.

If the surface is highly finished, the quantity $G \gg 1$ and the equilibrium density at the surface is essentially the same as at the axis. Helical surface waves can also be excited in this case but the mechanism by which these waves are generated is not connected with the gradient of the equilibrium density distribution.[11] This problem allows of a rigorous analytical solution. However, in discussing high-frequency stabilization there are appreciable difficulties because it is necessary to solve partial differential equations in three variables (r, z, t) with specified boundary conditions at the surface and at the ends.

In order to simplify the problem we shall use the approximate method (proposed by Glicksman [5] in the investigation of the helical instability in semiconductors); this approach gives good agreement with experiment when G > 1. The method consists of the following: the radial dependence of the perturbed quantities is assumed to be given

*$[\mathbf{v}_e\omega_{eH}] \equiv \mathbf{v}_e \times \omega_{eH}$.

by Bessel functions $J_1(\beta_1 r)$ where β_1 is chosen to make $J_1(\beta_1 r)$ vanish at the same point as $J_0(\beta_0 r)$.

Now, using the formalism of Kadomtsev and Nedospasov [3] for quasineutral perturbations ($n' = p'$) of the form

$$A' = A'(z, t) J_1(\beta_1 r) e^{i\varphi} \quad \text{(first mode)}, \tag{8}$$

after some lengthy calculations [5] from (1)—(4) we obtain the following set of equations for the small oscillations, these being the point of departure for the subsequent analysis:

$$\frac{\partial n'}{\partial t} + v_0 \frac{\partial n'}{\partial z} - D_e \frac{\partial^2 n'}{\partial z^2} + \left[D_e \beta_1^2 - \frac{Q\beta_0^2 (D_e - D_h)}{1 + 1/b} - iy_e L\beta_0^2 \frac{(D_e - D_h)}{1 + 1/b}\right] n' - b_e n_0 \left[-\frac{\partial^2 \varphi'}{\partial z^2} + (P\beta_1^2 - iy_e R\beta_0^2)\varphi'\right] = 0, \tag{9}$$

$$\frac{\partial n'}{\partial t} - \frac{v_0}{b}\frac{\partial n'}{\partial z} - D_h \frac{\partial^2 n'}{\partial z^2} + \left[D_h \beta_1^2 + \frac{Q\beta_0^2 (D_e - D_h)}{1 + b} - iy_h L\beta_0^2 \frac{(D_e - D_h)}{1 + b}\right] n' + b_h n_0 \left[-\frac{\partial^2 \varphi'}{\partial z^2} + (P\beta_1^2 + iy_h R\beta_0^2)\varphi'\right] = 0, \tag{10}$$

where $v_0 = -b_e E$, $E = E_{0c} + \tilde{E}\sin\omega_0 t$, E_{0c} is a constant longitudinal electric field; $\tilde{E}$ and ω_0 are the amplitude and frequency of the high-frequency component; $\beta_0 a$, $\beta_1 a$, L, Q, R, and T are constants that depend on the parameter G. These equations are derived under the assumption that $y_i = b_i H/c \ll 1$. The generation of carriers is neglected in the perturbation equations (9) and (10).

Using (9) and (10) we obtain an equation for $n'(z, t)$:

$$-2\frac{ibD_h}{R\beta_0^2(y_e + y_h)}\frac{\partial^4 n'}{\partial z^4} + \frac{\partial}{\partial t}\left\{\frac{i}{R\beta_0^2 y_h}\frac{\partial^2 n'}{\partial z^2} + \left[1 - \frac{i(P\beta_1^2 - iy_e R\beta_0^2)}{R\beta_0^2 y_h}\right] n'\right\} + \left[i\frac{D_e\beta_1^2}{R\beta_0^2 y_h} - \frac{ib(D_e - D_h)}{R\beta_0^2(y_e + y_h)}(\beta_1^2 + iy_h L\beta_0^2) + \frac{2iD_e(P\beta_1^2 - iy_e R\beta_0^2)}{R\beta_0^2(y_e + y_h)} - D_e\right]\frac{\partial^2 n'}{\partial z^2} + v_0\frac{\partial n'}{\partial z} + D_e\beta_1^2\left[1 - \frac{i(P\beta_1^2 - iy_e R\beta_0^2)}{R\beta_0^2 y_h}\right] n'$$

$$+ \frac{(D_e - D_h)}{1 + 1/b}\left[-Q\beta_0^2 - iy_e L\beta_0^2 + \frac{(P\beta_1^2 - iy_e R\beta_0^2)}{R\beta_0^2}\left(\frac{i\beta_1^2}{y_h} - L\beta_0^2\right)\right] n' = 0. \tag{11}$$

3. Since we are interested in the question of stabilization, we neglect in (11) all terms that have no bearing on the stabilization criterion (terms $\sim y_i$, with the exception of the current term). With this simplification (11) becomes

$$\hat{L}n' = 2D_e\left(\frac{\partial^4 n'}{\partial z^4} - P\beta_1^2\frac{\partial^2 n'}{\partial z^2}\right), \tag{12}$$

$$\hat{L} = (1 + b)\frac{\partial}{\partial t}\left(\frac{\partial^2}{\partial z^2} - P\beta_1^2\right) + 2D_e\beta_1^2\left(\frac{\partial^2}{\partial z^2} - P\beta_1^2\right) - iR\beta_0^2(y_e + y_h)v_0\frac{\partial}{\partial z}. \tag{12'}$$

We give values of the quantities $(\beta_0 a)^2$, $(\beta_1 a)^2$, $P(\beta_1 a)^2$, $R(\beta_0 a)^2$ for various values of the parameter G:

$\delta = n(a)/n(0)$:	0	0.2	0.5	0.8	0.95	0.98
$G = D_a/as$:	0	0.17	0.59	2.11	10	25.19
$(\beta_0\ a)^2$:	5.78	4.17	2.32	0.84	0.20	0.082
$(\beta_1\ a)^2$:	14.68	10.58	5.83	2.14	0.51	0.21
$R\ (\beta_0\ a)^2$:	3.85	2.74	1.39	0.45	0.10	0.041
$P\ (\beta_1\ a)^2$:	11.79	9.01	5.91	2.43	0.61	0.25

A table of these values is given by Glicksman [5] for values of the parameter $\delta = n(a)/n(0)$. However, the parameter G has more physical significance and for this reason we have included it in the table along with the corresponding values of the other parameters.

The relation in (12) is the starting point for investigating high-frequency stabilization. We note that the right side of (12) is $\sim a/L$ times the left side and when $L \gg a$ the right side can be treated as a perturbation.

If we write the dependence of perturbed quantities in the z-direction in the form of a plane wave $\exp(ik_z z)$, as is usually done in the theory of the screw instability, the time variation of the perturbed density is given by the equation

$$\frac{1}{n'}\frac{dn'}{dt} = -A^* + B^* v_0, \quad A^* = 2D_e\frac{\beta_1^2 + k_z^2}{1 + b},$$

$$B^* = \frac{R\beta_0^2 k_z y_h}{k_z^2 + P\beta_1^2}, \tag{13}$$

where A^* is a diffusion term, which stabilizes, while B^* is the destabilizing drift term. It is evident that (13) does not describe high-frequency stabilization: in the first half cycle the high-frequency field tends to drive the instability, but in the second half cycle it tends to stabilize it and the net effect vanishes when averages are taken over the high-frequency cycle. It will be shown below that the high-frequency stabilization is due primarily to the presence of waves reflected from the ends; these lead to the appearance of helical modes with different spatial period along the z-axis. The time correlation of a mode whose spatial period is comparable with the sample length L then leads to stabilization of the instability in the presence of the high-frequency field. Under these conditions the plane wave approximation, which holds when $L \gg \lambda_z$, no longer applies. In order to get a proper description of the effect we must solve (12) taking account of the boundary conditions at the ends.

The variables do not separate in (12) because v_0 depends on the time. Let us first consider the simpler equation

$$\hat{L}n' = 0, \tag{14}$$

in which the variables do separate: In (14) we take $n' = f(t)\Phi(z)$ in which case it is easy to obtain the following equation for the functions $f(t)$ and $\Phi(z)$:

$$\frac{1}{iR\beta_0^2 y_h v_0}\left(\frac{1}{f}\frac{df}{dt}+\frac{2D_h\beta_1^2}{1+1/b}\right) = \frac{d\Phi}{dz}\left[\frac{d^2\Phi}{dz^2}-P\beta_1^2\Phi\right]^{-1} = \alpha, \tag{15}$$

where α is a separation constant.

Using the boundary conditions

$$n'|_{z=0,\,L} = 0 \tag{16}$$

(it is assumed that the input and output are unperturbed since the development of the instability is due to volume processes) we can find the function Φ and the characteristic value α.

The equation for Φ is

$$\frac{d^2\Phi}{dz^2}-\frac{1}{\alpha}\frac{d\Phi}{dz}-P\beta_1^2\Phi = 0. \tag{17}$$

It is easy to solve this equation taking account of (16), the solution being obtained in terms of the characteristic functions (Φ) and the characteristic values (α):

$$\Phi_n(z) = e^{i\rho_n z}\sin\frac{\pi n}{L}z, \qquad \alpha_n = -\frac{i}{2\rho_n}, \tag{18}$$

where $n = 1, 2, \ldots;\ \rho_n = [P\beta_1^2 + (\pi n/L)^2]^{1/2}$.

The spatial period of the function $\Phi_n(z)$ in long samples

$$P\beta_1^2 \gg (\pi n/L)^2 \tag{19}$$

varies from 2a to 8a respectively as the parameter G varies from 0 to 10.

If (19) is satisfied the functions $\Phi_n(z)$ form an orthogonal set. If we keep the factor $\exp i[P\beta_1^2 + (\pi n/L)^2]^{1/2}z$, in the functions $\Phi_n(z)$ these functions are weakly orthogonal and the departure from orthogonality is given by $\sim a^2/L^2$. Hereinafter a characteristic function associated with a given value of n will be called the n-th mode. It is evident that the notion of a mode is not meaningful in long samples (19) because the variable $k_z = \pi n/L$ becomes continuous when $L \to \infty$.

The time variation of the n-th mode, as follows from (15), is given by

$$\frac{1}{f_n}\frac{df_n}{dt} = -\frac{2D_h\beta_1^2}{1+1/b}+\frac{R\beta_0^2 y_h v_0}{2\rho_n}. \tag{20}$$

This equation, like (13), does not describe high-frequency stabilization. The stabilization criterion for the n-th mode is given by

$$y_h v_0 < 4D_h\beta_1^2\rho_n / R\beta_0^2(1+1/b). \tag{21}$$

It is evident (see above) that when G increases the instability arises at lower values of $y_h v_0$. This is related to the fact that when G is increased the quantity $\delta = n(a)/n(0)$ is also increased, with a consequent reduction in the diffusional flux which acts to damp the screw instability.

An analysis of the more general equation (11) similar to that given above shows that at the stability limit the oscillation frequency

$$-\omega_{cr} = \frac{R\beta_0^2 D_h y_e}{1+b} \ll \gamma = \frac{R\beta_0^2 y_h v_0}{2\rho_n}, \tag{22}$$

where γ is the growth rate for the instability. Since $|\omega_{cr}| \ll \gamma$ the notion of an oscillation frequency is not meaningful at the stability limit in natural semiconductors, and one can only speak of the growth rate of the instability. As the order number of the mode (n) is increased the growth rate is reduced.

4. The solution of (12) can be written in the form of an expansion in characteristic functions of the operator $\hat{L}$:

$$n' = \sum_n C_n(t)\Phi_n(z). \tag{23}$$

In this representation the solution of (12) satisfies the boundary condition in (16). Taking account of (17) and (18) we write (12) in the form

$$\sum_n \Big\{-2b\rho_n\Big[\Big(1+\frac{1}{b}\Big)\frac{dC_n}{dt}+2D_h\beta_1^2(1+P)C_n\Big]$$
$$-16D_e\Big(\frac{\pi n}{L}\Big)^2\rho_n C_n+R\beta_0^2(y_e+y_h)v_0C_n\Big\}\rho_n\Phi_n$$
$$=\frac{i\pi}{L}\sum_n n\exp(i\rho_n z)\cos\frac{\pi n}{L}z\Big\{-2b\rho_n\Big[\Big(1+\frac{1}{b}\Big)\frac{dC_n}{dt}$$
$$+2D_h\beta_1^2(1+P)C_n\Big]-8D_e\rho_n\Big[\rho_n^2+\Big(\frac{\pi n}{L}\Big)^2\Big]C_n$$
$$+R\beta_0^2(y_e+y_h)v_0C_n\Big\}. \quad (24)$$

It is evident that as $L \to \infty$ (19) the change in the function n' in time is given by (20), which does not describe high-frequency stabilization. Thus, high-frequency stabilization does not operate in long samples, as is verified by the following calculations.

In (24) we consider the first two modes ($n = 1, 2$), which have the highest growth rates. The solution of (24) is carried out by perturbation methods, in which we neglect all C_n for which $n > 2$.

Let us require that the system of functions

$$\Phi_1=\exp(i\rho_1 z)\sin\frac{\pi}{L}z,\qquad \Phi_2=\exp(i\rho_2 z)\sin\frac{2\pi}{L}z, \quad (25)$$

be orthogonal to the system of functions ψ:

$$\psi_1=\exp(-i\rho_2 z)\sin\frac{\pi}{L}z,$$
$$\psi_2=\exp(-i\rho_1 z)\sin\frac{2\pi}{L}z, \quad (25')$$

so that

$$\int_0^L \psi_1\Phi_1 dz=\frac{\exp i(\rho_1-\rho_2)L-1}{2i(\rho_1-\rho_2)}=A, \quad (26)$$
$$\int_0^L \psi_2\Phi_2 dz=\frac{\exp i(\rho_2-\rho_1)L-1}{2i(\rho_2-\rho_1)}=B, \quad (27)$$
$$\int_0^L \psi_1\Phi_2 dz=\int_0^L \psi_2\Phi_1 dz=0. \quad (28)$$

In long samples $A, B \approx L/2$: For a "dirty" surface $G \sim 0$ when $L/\alpha > 5$ and for a "clean" surface $G \approx 10$ when $L/\alpha > 10$.

Multiplying (24) respectively by ψ_1 and ψ_2 and integrating with respect to z from 0 to L we obtain two equations for the coefficients C_1 and C_2 which describe the time dependence of the perturbed quantities:

$$\{-2(1+b)\rho_1\dot{C}_1-4D_e[4\rho_1^2+(1-3P)\beta_1^2]\rho_1C_1$$
$$+R\beta_0^2(y_e+y_h)v_0C_1\}A\rho_1+{}^4/_3 i\{-2(1+b)\rho_2\dot{C}_2$$
$$-4D_e\rho_2[4\rho_2^2+(1-P)\beta_1^2]C_2$$
$$+R\beta_0^2(y_e+y_h)v_0C_2\}=0, \quad (29)$$

$$\{-2(1+b)\rho_2\dot{C}_2-4D_e[4\rho_2^2+(1-3P)\beta_1^2]\rho_2C_2$$
$$+R\beta_0^2(y_e+y_h)v_0C_2\}B\rho_2-{}^4/_3 i\{-2(1+b)\rho_1\dot{C}_1$$
$$-4D_e\rho_1[4\rho_1^2+(1-P)\beta_1^2]C_1$$
$$+R\beta_0^2(y_e+y_h)v_0C_1\}=0, \quad (30)$$

where $\dot{C} = dC/dt$.

It is evident from (29) and (30) that the functions C_1 and C_2 are shifted in time phase. In long samples this shift is approximately $\pi/2$. The phase shift arises because of the reflected waves. There is no correlation between C_1 and C_2 in long samples (19) and each of them varies in time in accordance with a first-order equation

$$\frac{\dot{C}}{C}=-\frac{2D_h\beta_1^2}{1+1/b}+\frac{R\beta_0^2y_hv_0}{2\beta_1P^{1/2}} \quad (31)$$

which does not allow a stabilization effect.

When mode correlation does exist, i.e., when

$$P\beta_1^2 \sim (\pi/L)^2,\ (2\pi/L)^2, \quad (32)$$

the presence of a phase shift in time with the application of the high-frequency field can lead to a stabilizing effect which we will consider qualitatively for the phase shift $\pi/2$. In the first half cycle the high-frequency field amplifies the first mode and weakens the second; the pattern is reversed on the second half cycle. Thus, the effect of stabilization and destabilization due to the high-frequency field exists at each instant of time, whereas in (13) these effects are shifted with respect to each other at the frequency of the variable component. The total effect of the high-frequency field on the screw instability described by (29) and (30) can be found from the generalized Hill equation which, in turn, can be developed from the equations for the coefficients C_1 and C_2 starting from (29) and (30). It should be noted that in samples with clean surfaces the condition for strong correlation of the modes (32) is satisfied over a wider range of variation of sample length L/a; hence, the stabilization effect should be more pronounced in such samples. (This assumption will be verified by further calculation.)

5. Solving the system of equations (29) and (30), which are first order in each of the functions C_1 and C_2, we obtain a second-order equation of the form

$$\ddot{C}_1+2\varepsilon\dot{C}_1+\varkappa C_1=0, \quad (33)$$

where

$$2\varepsilon=\frac{D_e a^{-2}}{1+b}f_1\Big(\frac{L}{a}\Big)-\frac{v_0y_h}{a}f_2\Big(\frac{L}{a}\Big), \quad (34)$$

$$\varkappa = \left(\frac{D_e a^{-2}}{1+b}\right)^2 \chi_1\left(\frac{L}{a}\right) - \frac{D_e a^{-2}}{1+b}\frac{v_0 y_h}{a}\chi_2\left(\frac{L}{a}\right) + \frac{v_0^2 y_h^2}{a^2}\chi_3\left(\frac{L}{a}\right) - \frac{y_h}{a}\frac{dv_0}{dt}\chi_4\left(\frac{L}{a}\right). \quad (35)$$

The coefficients f_1, f_2, χ_1, χ_2, χ_3, and χ_4 are functions of the dimensionless sample length (L/α) only. Expressions for these coefficients are given in the Appendix. The coefficients ϵ and κ in the equation for the function C_2 can be obtained by interchanging ρ_1 and ρ_2 in the coefficients f and χ given above.

Hereinafter we will only consider (33), which describes the time variation of the most dangerous mode, the first. The solution of (33) is written in the form

$$C_1 = \text{const}\cdot\exp\{-\textstyle\int \varepsilon\, dt\}\, u(t), \qquad \varepsilon = \varepsilon_c + \tilde{\varepsilon}\sin\omega_0 t, \quad (36)$$

where u(t) satisfies the equation

$$\ddot{u} + (\varkappa - \varepsilon^2 - \dot{\varepsilon})u = 0. \quad (37)$$

It is evident that high-frequency stabilization can be described by (37). When $L \to \infty$ the quantity $\kappa - \epsilon^2 - \dot{\epsilon} \to 0$ and the time variation of the function C_1 is given by an exponential factor which agrees with (31). As we have noted above this equation does not contain high-frequency stabilization.

High-frequency stabilization can be realized only when the development of the instability in the absence of the high frequency field is determined by the time behavior of the function u i.e., stabilization can only be realized if

$$\varepsilon_c > 0, \qquad \varkappa_c < 0. \quad (38)$$

The first condition means that the perturbations are damped if the function u does not grow; the second indicates that the instability is excited in the absence of the high-frequency field. Using (34) and (35) we can reduce (38) to the following inequalities:

$$\varepsilon_c > 0, \quad \theta < f_1/f_2; \quad (39)$$

$$\varkappa_c < 0, \quad \frac{1}{2\chi_3}[\chi_2 - (\chi_2^2 - 4\chi_1\chi_3)^{1/2}] < \theta < \frac{1}{2\chi_3}[\chi_2 + (\chi_2^2 - 4\chi_1\chi_3)^{1/2}]; \quad (40)$$

where the quantity θ is given by

$$\theta = \frac{v_{0c} y_h}{a}\left(\frac{D_e a^{-2}}{1+b}\right)^{-1}. \quad (41)$$

Since

$$(2\chi_3)^{-1}[\chi_2 + (\chi_2^2 - 4\chi_1\chi_3)^{1/2}] > f_1/f_2,$$

(38) can be reduced to the inequality

$$\frac{f_1}{f_2} > \theta > \frac{1}{2\chi_3}[\chi_2 - (\chi_2^2 - 4\chi_1\chi_3)^{1/2}]. \quad (42)$$

The condition in (42) determines the allowable values of θ for which high-frequency stabilization is possible. In Fig. 1 this relation is shown in the form of a cross-hatched region for various values of L/a. The narrow band corresponds to a dirty surface (G = 0) and the wide band to a clean surface (G = 10). It is evident from this figure that high-frequency stabilization can be achieved more easily in samples characterized by $G \gg 1$.

As L/a increases both regions tend to vanish. Thus, it is more difficult to satisfy the condition for high-frequency stabilization (42) as L/a increases.

We now write (37) in the form

$$\frac{d^2u}{d\tau^2} + \left(\theta_0 + 2\theta_{1s}\sin 2\tau + 2\sum_{\nu=1}^{2}\theta_{\nu c}\cos 2\nu\tau\right)u = 0, \quad (43)$$

where

$$\theta_0 = -\frac{4}{\omega_0^2}\left[\left(\frac{D_e a^{-2}}{1+b}\right)^2\left(\frac{1}{4}f_1^2 - \chi_1\right) + \frac{v_{0c}y_h}{a}\left(\frac{D_e a^{-2}}{1+b}\right) \times \left(\chi_2 - \frac{f_1 f_2}{2}\right) + \frac{y_h^2}{a^2}\left(\frac{1}{4}f_2^2 - \chi_3\right)\left(v_{0c}^2 + \frac{\tilde{v}_0^2}{2}\right)\right],$$

$$\theta_{1s} = -\frac{2}{\omega_0^2}\tilde{v}_0\frac{y_h}{a}\left[2v_{0c}\frac{y_h}{a}\left(\frac{1}{4}f_2^2 - \chi_3\right) + \left(\frac{D_e a^{-2}}{1+b}\right)\left(\chi_2 - \frac{f_1 f_2}{2}\right)\right],$$

$$\theta_{1c} = -\frac{2}{\omega_0}\frac{y_h}{a}\tilde{v}_0\sqrt{\frac{1}{4}f_2^2 - \chi_3}, \qquad \frac{1}{4}f_1^2 - \chi_1 > 0,$$

$$\theta_{2c} = \frac{\tilde{v}_0^2 y_h^2}{\omega_0^2 a^2}\left(\frac{1}{4}f_2^2 - \chi_3\right), \qquad \chi_2 - \frac{f_1 f_2}{2} > 0,$$

$$\tau = \frac{\omega_0 t}{2}, \qquad \frac{1}{4}f_2^2 - \chi_3 > 0.$$

This equation (43) is the generalized Hill equation.[15]

When

$$|\theta_0| \ll 1 \quad (44)$$

the first region of stable solutions of (43) is given by the inequality

$$\theta_1 - 1 < |\theta_0| < \frac{\theta_1^2}{2} + \frac{\theta_{2c}^2}{8}, \quad (45)$$

where $\theta_1 = \sqrt{\theta_{1c}^2 + \theta_{1s}^2}$.

The condition in (44) determines the frequency of the high-frequency field which is capable of stabilization while the inequality in (45) gives the

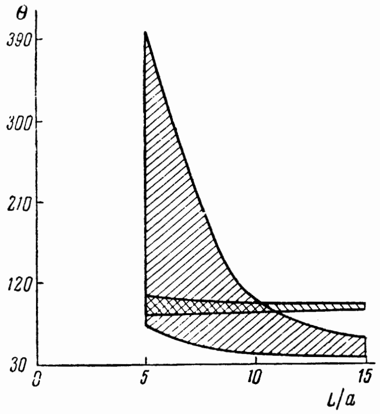

FIG. 1

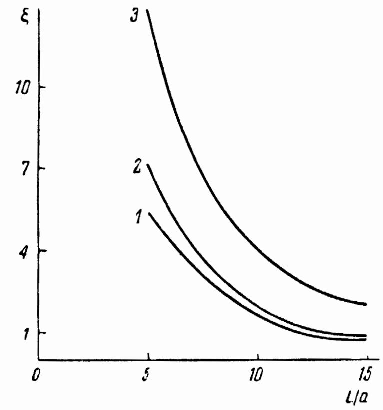

FIG. 2. Curve 1 corresponds to G = 10, $\theta = \theta_{min}$, curve 2–G = 10, $\theta = \theta_{max}$, curve 3 – G = 10.

boundaries of the modulation coefficient ($\eta = \tilde{v}_0/v_{0c}$) for which stabilization is possible. Under the assumption that $\eta \lesssim 1$ (44) can be written in the form

$$\omega_0 \gg 2\left(\frac{D_e a^{-2}}{1+b}\right)\left[\frac{1}{4}f_1^2 - \chi_1 + \theta\left(\chi_2 - \frac{f_1 f_2}{2}\right) + \theta^2\left(\frac{1}{4}f_2^2 - \chi_3\right)\right]^{1/2} = \gamma_0. \quad (46)$$

The quantity γ_0 diminishes with increasing L/a; it does not vary appreciably with θ for a clean surface and is essentially independent of θ for a dirty surface. Curves showing the dependence of the quantity $\xi = \frac{1}{2}\gamma_0[D_e/a^2(1+b)]^{-1}$ on L/a are given in Fig. 2 for the cases G = 0 and G = 10 ($\theta = \theta_{min}$ and $\theta = \theta_{max}$). The values θ_{min} and θ_{max} correspond to the lower and upper boundaries of a region of allowable values of θ (cf. Fig. 1).

For germanium samples at room temperature the condition in (46) with ($D_e \approx 10^2$ cm²/sec, b ≈ 2, a = 0.05 cm) taking account of the dependence of γ_0 on L/a is given by

$$\omega_0 \gg 0.5\text{—}3\cdot 10^5\ \text{sec}^{-1}. \quad (47)$$

Calculations show that the left side of (45) is always satisfied while the right side can be reduced approximately to the following condition for the modulation coefficient η ($\omega_0 = l\gamma_0$):

$$\eta > \sqrt{2}\frac{l}{\theta^2}\left(\frac{f_2^2}{4} - \chi_3\right)^{1/2}\left[\frac{f_1^2}{4} - \chi_1 + \theta\left(\chi_2 - \frac{f_1 f_2}{2}\right) + \theta^2\left(\frac{f_2^2}{4} - \chi_3\right)\right]\left[\frac{f_2^2}{4} - \chi_3 + \frac{1}{2\theta}\left(\chi_2 - \frac{f_1 f_2}{2}\right)\right]^{-1}. \quad (48)$$

This expression holds if the modulation frequency is not too high: for the case of a dirty surface l < 15 – 40 as L/a varies from 5 to 15; for the case of a clean surface l < 30 – 60 as L/a varies over the same range. The limitation on the modulation frequency arises from the fact that we have gone from the rigorous expression for the stabilizing modulation coefficient η_c, obtained from (45), to the form in (48), which is simple and convenient for calculation.

A calculation of the lower limits of the modulation coefficient η_c as the function of sample length has been carried out using (48) for the cases

1) $G = 0, \quad \theta = \theta_{min}, \quad \theta = \theta_{max};$

2) $G = 10, \quad \theta = \theta_{min}, \quad \theta = \theta_{max}.$

In both cases l = 3. The results of the calculation are shown in Fig. 3.

In each of these cases the values of the stabilizing modulation coefficients lie above the corresponding curve. It is evident from (48) that the stabilization modulation coefficient η_c increases as the modulation frequency increases (it being

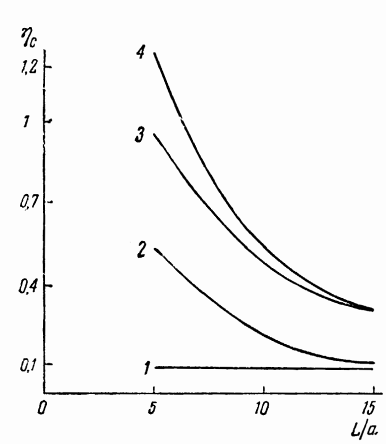

FIG. 3. The curves apply to the following values of the parameters: 1) G = 10, $\theta = \theta_{max}$; 2) G = 10, $\theta = \theta_{min}$; 3) G = 0, $\theta = \theta_{max}$; 4) G = 0, $\theta = \theta_{min}$.

assumed that (46) is satisfied in all cases). A similar situation is characteristic in the analysis of the dynamic stability of the inverted pendulum[14] and is due to the reaction in the high-frequency correction, which goes as ω_0^{-2}, when one carries out the averaging procedure over the high-frequency component. It is easy to find the modulation coefficient η_c required for an arbitrary modulation frequency by using the results of the calculation (Fig. 3) and the relation in (48). As θ is reduced [within the allowable range (42)] the required modulation coefficient η_c increases (this effect is very weak in long samples); when L/a increases (for a fixed value of ω_0/γ_0) the modulation coefficient is reduced. Experimental verification of the dependence of η_c on L/a requires that the generated frequency be changed in such a way as to keep the quantity ω_0/γ_0 constant. It should be noted that the modulation coefficient η_c in clean samples is appreciably smaller than in dirty samples, assuming all other conditions to remain unchanged.

The above calculations show that high-frequency stabilization of the screw instability in semiconductors should be realized in short samples characterized by small rates of carrier surface recombination ($G \gg 1$) over a specific range of variation of θ (42).

The criteria in (42), (47) and (48) are in good agreement with the experimental results on high-frequency stabilization of the screw instability in germanium samples obtained by Dubovoĭ and Shanskiĭ.[12]

6. Great interest attaches to the experimental observation of helical modes in the sample. One possible means of doing this, indicated to the author by V. F. Shanskiĭ consists of measuring the spatial distribution (along the z-axis) of the resultant signal due to the superposition of correlated modes which are shifted in time phase. We compute this distribution for the case of the first two modes: in accordance with (25) these are described by

$$\Phi_1(z, t) = A_0 \cos \beta_1 P^{1/2} z \sin \frac{\pi}{L} z \sin \omega t,$$

$$\Phi_2(z, t) = \frac{A_0}{m} \cos \beta_1 P^{1/2} z \sin \frac{2\pi}{L} z \sin(\omega t + \varphi), \quad (49)$$

where φ is the phase shift in time. The parameter m gives the mode amplitude and ratio.

The resulting signal from the superposition of these two modes is

$$\Phi = A_0 I(z) \cos \beta_1 P^{1/2} z \sin(\omega t + \varphi_0), \quad (50)$$

where

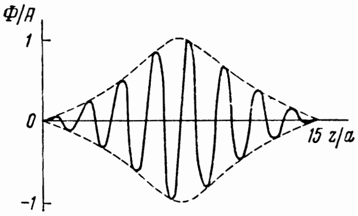

FIG. 4

$$I(z) = g(z) \sin\left(\frac{\pi}{L} z\right) \left[1 + \frac{4\cos^2\left(\frac{\pi}{L} z\right) \sin^2 \varphi}{m^2 g^2(z)}\right]^{-1/2}$$

$$\tan \varphi_0 = \frac{2}{m g(z)} \cos\left(\frac{\pi}{L} z\right) \sin \varphi,$$

$$g(z) = 1 + \frac{2}{m} \cos\left(\frac{\pi}{L} z\right) \cos \varphi.$$

The spatial distribution of the resulting signal is given in Fig. 4 for the case G = 0, L/a = 15, m = 1, $\varphi = \pi/2$. The shape of the envelope is given by the function I(z).

It is evident that this distribution is symmetric with respect to the center of the sample when $\varphi = \pi/2$, with a clearly defined peak at the center. The peak spreads as m increases. The same pattern is observed for a clean surface, but the period of the spatial oscillations becomes larger.

The formalism developed in this work can be applied to the study of high-frequency stabilization of the screw instability in a positive column. A subsequent paper will be devoted to this topic.

In conclusion I wish to express my gratitude to B. B. Kadomtsev for proposing the problem and for guidance, to Academician M. A. Leontovich for a number of valuable comments, and to L. V. Dubovoĭ, I. M. Roĭfe and V. F. Shanskiĭ for fruitful discussions of various questions encountered in the course of the work.

APPENDIX

The expressions for the coefficients f and χ are given by

$$f_1 = 2[XY + Z - 2PAB\rho_1^2(a\beta_1)^2 Y],$$

$$f_2 = \frac{1}{2} \frac{R(a\beta_0)^2}{a\rho_1} \left[1 + \left(\frac{\rho_1}{\rho_2}\right)^{1/2}\right],$$

$$\chi_1 = -8PAB\rho_1^2(a\beta_1)^2[4(a\rho_1)^2$$

$$+ (1 - 3P)(a\beta_1)^2]Y + 4XYZ,$$

$$\chi_2 = -2PRAB\beta_1^2(a\beta_0)^2(a\rho_1)Y + \frac{R(a\beta_0)^2}{a\rho_2}XY + \frac{R(a\beta_0)^2}{a\rho_1}Z,$$

$$\chi_3 = \frac{1}{4}\frac{(Ra^2\beta_0^2)^2}{a^2(\rho_1\rho_2)^{1/2}}, \qquad \chi_4 = \frac{1}{2}\frac{R(a\beta_0)^2}{a\rho_1};$$

here

$$X = AB\rho_1^2[4(a\rho_1)^2 + (1-3P)(a\beta_1)^2] - 1.78(\rho_1/\rho_2)^{1/2}[4(a\rho_1)^2 + (1-P)(a\beta_1)^2],$$

$$Y = \left[AB\rho_1^2 - 1.78\left(\frac{\rho_1}{\rho_2}\right)^{1/2}\right]^{-1},$$

$$Z = 4(a\rho_2)^2 + (1-P)(a\beta_1)^2.$$

[1] B. Lehnert, Proc. of the 2-nd International Conference on the Peaceful Uses of Atomic Energy, Geneva, 1958.

[2] Yu. L. Ivanov and S. M. Ryvkin, ZhTF **28**, 774 (1958), Soviet Phys. Tech. Phys. 3, 722 (1958).

[3] B. B. Kadomtsev and A. V. Nedospasov, J. Nucl. Energy Part C 1, 230 (1960).

[4] Allen, Paulikas and Pyle, Phys. Rev. Letters 5, 409 (1960); G. A. Paulikas and R. V. Pyle, Phys. Fluids 5, 348 (1962); V. L. Vdovin and A. V. Nedospasov, ZhTF 32, 817 (1962), Soviet Phys.-Tech. Phys. 7, 598 (1963).

[5] M. Glicksman, Phys. Rev. **124**, 1655 (1961).

[6] J. Bok and R. Veilex, Compt. rend **248**, 2300 (1959); R. D. Larrabee and M. C. Steele, J. Appl. Phys. **31**, 1519 (1960).

[7] B. Ancker-Johnson, Proc. of the International Conference on the Physics of Semiconductors, London, 1962.

[8] Okamoto, Koike and Tosima, J. Phys. Soc. Japan **17**, 804 (1962).

[9] L. E. Gurevich and I. V. Ioffe, FTT **4**, 2641 (1962), Soviet Phys.-Solid State 4, 1938 (1963); FTT **6**, 445 (1964), Soviet Phys. Solid State **6**, 354 (1964).

[10] Ø. Holter, Phys. Rev. **129**, 2548 (1963).

[11] C. E. Hurwitz and A. L. McWhorter, Phys. Rev. **134A**, 1033 (1964).

[12] L. V. Dubovoi and V. F. Shanskiĭ, JETP **48**, 800 (1965), Soviet Phys. JETP **21**, 530 (1965).

[13] H. F. Rugge and R. V. Pyle, Phys. Fluids **7**, 754 (1964).

[14] S. M. Osovets, JETP **39**, 311 (1960), Soviet Phys. JETP **12**, 221 (1961); N. A. Bobyrev and O. I. Fedyanin, ZhTF **32**, 823 (1962) Soviet Phys. Tech. Phys. **7**, 602 (1963); ZhTF **33**, 1187 (1963), Soviet Phys. Tech. Phys. **8**, 887 (1964).

[15] T. Hayashi, Forced Oscillations in Nonlinear Systems, Nippon Publishing Co., Osaka, 1953.

Translated by H. Lashinsky
201